

Structure–Reactivity Relationships of Buchwald-Type Phosphines in Nickel-Catalyzed Cross-Couplings

Samuel H. Newman-Stonebraker, Jason Y. Wang, Philip D. Jeffrey, and Abigail G. Doyle*



Cite This: <https://doi.org/10.1021/jacs.2c09840>



Read Online

ACCESS |



Metrics & More

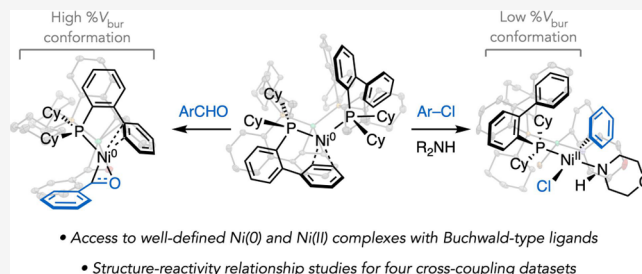


Article Recommendations



Supporting Information

ABSTRACT: The dialkyl-*ortho*-biaryl class of phosphines, commonly known as Buchwald-type ligands, are among the most important phosphines in Pd-catalyzed cross-coupling. These ligands have also been successfully applied to several synthetically valuable Ni-catalyzed cross-coupling methodologies and, as demonstrated in this work, are top performing ligands in Ni-catalyzed Suzuki Miyaura Coupling (SMC) and C–N coupling reactions, even outperforming commonly employed bisphosphines like dppf in many circumstances. However, little is known about their structure–reactivity relationships (SRRs) with Ni, and limited examples of well-defined, catalytically relevant Ni complexes with Buchwald-type ligands exist. In this work, we report the analysis of Buchwald-type phosphine SRRs in four representative Ni-catalyzed cross-coupling reactions. Our study was guided by data-driven classification analysis, which together with mechanistic organometallic studies of structurally characterized Ni(0), Ni(I), and Ni(II) complexes allowed us to rationalize reactivity patterns in catalysis. Overall, we expect that this study will serve as a platform for further exploration of this ligand class in organonickel chemistry as well as in the development of new Ni-catalyzed cross-coupling methodologies.



INTRODUCTION

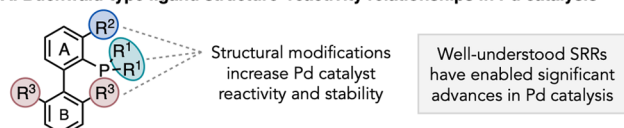
Transition metal-catalyzed cross-couplings are among the most practical and widely used bond-forming reactions in the construction of small molecules.^{1,2} The modern-day success of these methodologies is due in large part to ancillary ligand and precatalyst development, aided by thorough mechanistic investigations.^{1,3} For Pd-catalyzed cross-couplings, the dialkyl-*ortho*-biaryl phosphines developed by Buchwald, Beller, and others have emerged as the ligand class of choice for many C–C and C–N bond-forming transformations.^{4–8} Extensive mechanistic studies have been carried out to elucidate the structure–reactivity relationships (SRRs) of these phosphines with Pd (Figure 1A).^{6,9–13} In brief, because of their large size, Buchwald-type ligands promote the formation of highly reactive monoligated (L₁)¹⁴ Pd by positioning the “B ring” within the metal’s first coordination sphere, which prevents binding of multiple ancillary ligands. Additionally, they also can stabilize the unsaturated Pd center via interactions with the biaryl π -system (a pseudobidentate binding mode).^{11,12,15,16} Most members of this ligand class are also characterized by a high degree of conformational flexibility, resulting in a wide range of attainable steric environments around the metal center (Figure 1B),^{12,13} which can be limited by introducing groups on the A ring or increasing the size of the alkyl groups bound to phosphorus.^{13,17} Overall, the design elements of these ligands promote challenging elementary steps while minimizing off-cycle speciation and allow for deactivated

electrophiles such as aryl chlorides to be employed in catalysis with high levels of efficiency.^{6,11}

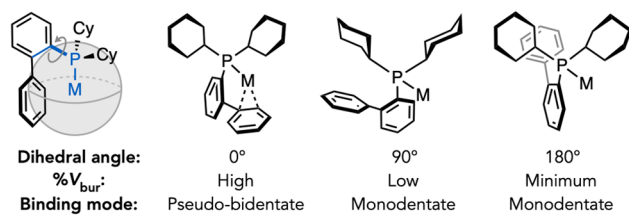
Over the past decade, Buchwald-type phosphines have also found successful application in a number of synthetically valuable Ni-catalyzed cross-coupling methodologies (Figure 1C).^{18–26} One of the first reports came from our laboratory in 2011 with the development of a Ni-catalyzed cross-coupling of styrenyl epoxides and boronic acids, where BrettPhos was identified to be the most effective ligand in the transformation.¹⁹ The Watson and Cruden laboratories have also reported the use of Buchwald-type phosphines in Ni-catalyzed cross-coupling reactions of naphthyl pseudohalides.^{20,21} More recently, researchers at Bristol Myers Squibb identified CyJohnPhos as the most effective ligand for the Ni-catalyzed borylation of aryl halides, with other examples of the ligand class among the top performers.²² Additionally, in a recent collaborative project carried out by our laboratory, the Sigman lab, and Merck & Co., Inc., we identified certain Buchwald-type phosphines as top performing among 90 diverse monophosphines for several Suzuki–Miyaura Coupling

Received: September 15, 2022

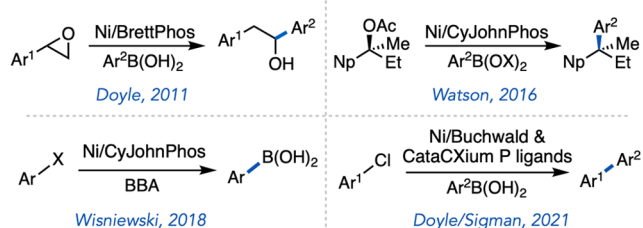
A. Buchwald-type ligand structure–reactivity relationships in Pd catalysis



B. Conformational flexibility and binding modes of Buchwald-type ligands



C. Examples of Buchwald-type ligands in Ni catalysis



D. This work

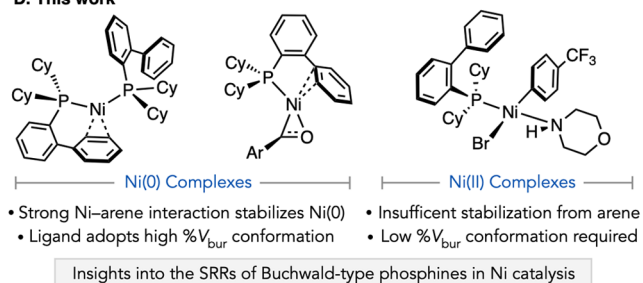


Figure 1. Introduction.

(SMC) reactions of aryl chlorides,²⁶ and even outcompete commonly used bisphosphines.

While these examples illustrate that Buchwald ligands are capable of imparting desirable reactivity in Ni-catalyzed methodologies, little is known about their SRRs in Ni catalysis or how their unique structure and binding modes interface with Ni more generally. Few computational studies have included Buchwald phosphines in their analyses, and the focus was not on the ligand class specifically.^{27,28} Nicasio and coworkers have structurally characterized dialkylterphenyl phosphines on Ni; these ligands share certain attributes with Buchwald-type ligands.^{29–31} However, to the best of our knowledge, only one example exists in the literature of a structurally characterized Ni complex bound by a Buchwald phosphine: an off-cycle, cyclometalated adduct of BrettPhos formed during the cross-coupling of styrenyl epoxides.¹⁹ Given the scarcity of relevant studies, insights into the SRRs and mechanism of Buchwald and CataCXium P phosphines in Ni catalysis, along with access to well-defined Ni complexes bearing these ligands, would be of great value both in the discovery of new methodologies and in the further understanding/optimization of existing ones.

Herein, we report findings into the mechanism and SRRs of Buchwald-type phosphines in Ni cross-coupling catalysis, guided by data science-driven classification analysis, organometallic studies, and density functional theory (DFT). Five Ni-

catalyzed cross-coupling datasets where Buchwald-type phosphines are active to varying degrees were used as case studies to explore catalyst structure and mechanism. Each of these cases provided insights into different elementary organometallic processes, and the identification of percent buried volume (% V_{bur}) reactivity threshold in several of these datasets allowed for the interrogation of the specific ligand structural components that led to active (and inactive) catalysts.^{26,32–34} Structural characterization and reactivity studies of new well-defined Ni complexes bound by Buchwald and CataCXium P phosphines were carried out for each of the reactions, allowing us to rationalize the observed reactivity patterns (Figure 1D). The findings of this study should serve as a platform for the further exploration of organonickel chemistry with Buchwald-type ligands, and the principles relating ligand structure to speciation and reactivity will further enable the rational use of this ligand class in Ni catalysis.

RESULTS AND DISCUSSION

% V_{bur} Reactivity Thresholds and Catalytic Case Studies. At the outset of this study, we sought to use molecular features to describe the structure of Buchwald-type ligands in relation to their reactivity in Ni-catalyzed cross-couplings. To this end, Gensch et al. recently developed a comprehensive organophosphorus descriptor database, *kraken*, which contains conformationally informative electronic, steric, and whole-molecule DFT descriptors for 1558 unique monophosphines, including Buchwald-type ligands.³⁵ The descriptors generated for each ligand include the minimum, maximum, and Boltzmann-weighted average value for each feature across the phosphine's energetically accessible conformational ensemble, allowing for accurate representations of ligand structure relevant in coordination chemistry and organometallic catalysis (see the Supporting Information for more information). In our 2021 collaborative study with the Sigman lab and Merck & Co., Inc., we found that one of these conformationally representative descriptors, minimum percent buried volume (% V_{bur} (*min*)), enabled the discovery of reactivity threshold in Ni- and Pd-catalyzed cross-coupling datasets. These univariate reactivity cliffs were defined by a threshold value, wherein for Ni, all monodentate phosphine ligands that had a % V_{bur} (*min*) greater than this value afforded no reactivity.²⁶ Mechanistic studies revealed that a given phosphine's % V_{bur} (*min*) was linked to the formation of monoligated (L_1M) vs bisligated (L_2M) catalysts,¹⁴ wherein the former was generally required for successful Pd catalysis and the latter for successful Ni catalysis.^{3,26,36}

While this workflow could be used to predict and rationalize the ligation state of the metal with Buchwald-type phosphines (typically L_1), it was not effective at capturing the catalytic reactivity behavior of these ligands. The large range of % V_{bur} values (Figure 2) and different binding modes (Figure 1B) attainable by these ligands explained their complex behavior in the Pd-catalyzed case studies,³⁷ but an understanding of their activity was less obvious for Ni. Indeed, despite Buchwald-type ligands preferentially forming L_1Ni (substrate) species, members of the class with relatively low % V_{bur} (*min*) values were the best or second-best performing ligands for many of the SMCs studied (see the Supporting Information for histograms), even outperforming commonly used bisphosphines like dppe.^{38–40} No other phosphines that enforced L_1Ni (substrate)¹⁴ ligation states were found to be successful ligands. These observations

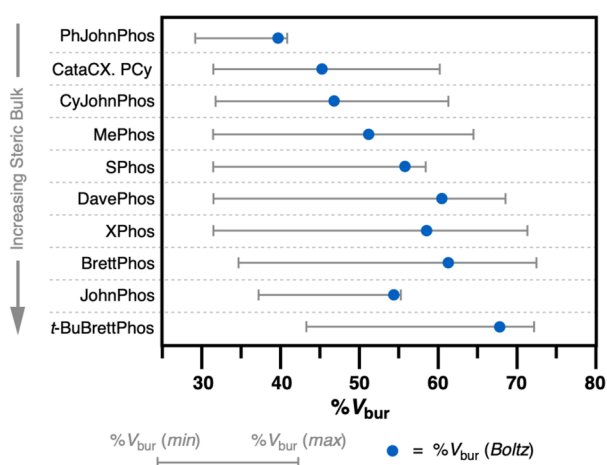


Figure 2. $\%V_{\text{bur}}$ range for select Buchwald and CataCXium P phosphines as defined by $\%V_{\text{bur}}(\text{min})$ and $\%V_{\text{bur}}(\text{max})$ from the *kraken* database. The Boltzmann-weighted $\%V_{\text{bur}}$ value is shown on the range as a blue dot. See the [Supporting Information](#) for more information.

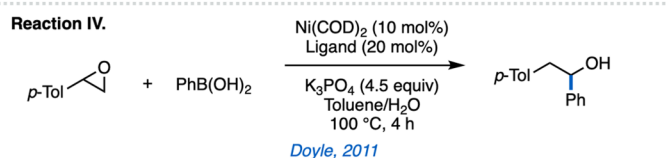
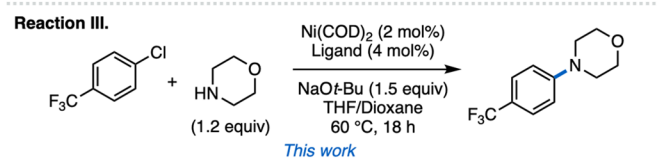
raised questions about how Buchwald-type ligands interact with Ni from both a structural and catalytic perspective.

Guided by reactivity threshold analysis, we assembled four Ni-catalyzed cross-coupling datasets as case studies (Figure 3A, Reactions I–IV), combining previously published (Reactions I, II, IV)^{19,26} and newly collected (Reaction III) datasets,

wherein at least some Buchwald-type ligands were found to promote reactivity. These case studies, consisting of Csp^2 – Csp^2 Suzuki–Miyaura couplings (Reactions I and II), a Csp^2 –N coupling (Reaction III) of aryl chlorides, and a Csp^3 – Csp^2 SMC of *p*-tol styrene oxide (Reaction IV), highlight several different reactivity patterns of Buchwald-type ligands in Ni catalysis, especially in the context of $\%V_{\text{bur}}(\text{min})$ thresholds.

Case Study 1: Investigation of Ni(0) and Oxidative Addition in Suzuki–Miyaura Couplings. In the first case study, we examined Reaction I, an electronically mismatched SMC, wherein only four of the smallest Buchwald-type ligands screened (CyJohnPhos, CataCXium PCy, CataCXium PInCy, and CataCXium POMEcy) promoted reactivity. Notably, CataCXium PCy was the second best of 90 monophosphines screened in this reaction. These four ligands fell on the left (reactive) side of a 32% $V_{\text{bur}}(\text{min})$ reactivity threshold (Figure 3B), but the descriptor alone did not distinguish the ligands from inactive Buchwald-type ligands with similar $\%V_{\text{bur}}(\text{min})$ values, such as SPhos and XPhos. This is in contrast with Reaction II, where *all* Buchwald-type ligands screened with $\%V_{\text{bur}}(\text{min})$ values less than 32% were reactive above the control with no phosphine ligand (Figure 3B). Because the reaction partners in Reaction II are activated, the difference in ligand response between Reactions I and II suggested to us that the four active ligands in Reaction I enabled the formation of a Ni species that could undergo a challenging elementary step of the catalytic cycle.

A. Ni-catalyzed cross-coupling reaction case studies



B. $\%V_{\text{bur}}(\text{min})$ reactivity thresholds in Ni-catalyzed cross-coupling datasets highlighting Buchwald-type phosphines

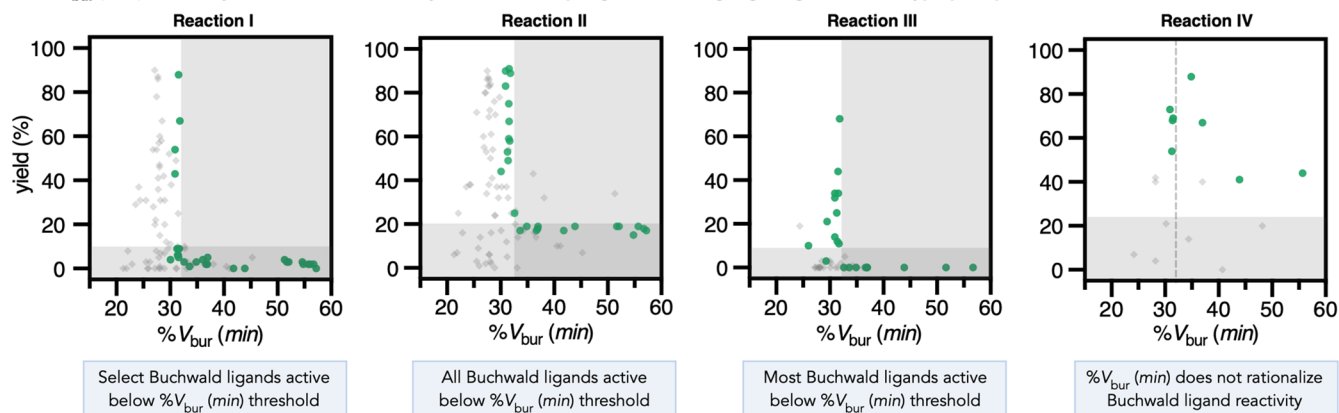


Figure 3. (A) Catalytic reactions studied. See the [Supporting Information](#) for complete reaction conditions and procedures. (B) Buchwald-type ligand reactivity threshold analysis. Green circles are Buchwald-type ligands. Gray diamonds (faded) are all ligands other than Buchwald-type screened. The location of the horizontal gray box represents either background reactivity of Ni(COD)₂ (i.e., with no phosphine ligand) or 10% yield, whichever is higher. The location of the vertical gray box represents the $\%V_{\text{bur}}(\text{min})$ threshold decision. No threshold was located for Reaction IV.

Examining Reaction **Ib**, a SMC employing the same 4-chloroanisole electrophile as Reaction **I** but an electron neutral phenyl boronic acid (Scheme 1), we found that the same four

Scheme 1. Ni-Catalyzed SMC Reaction **Ib**



ligands as those identified in Reaction **I** were the only reactive Buchwald-type phosphines (see the Supporting Information for threshold analysis). This observation suggests that the challenging step is oxidative addition into the electron-rich electrophile.^{41,42} Therefore, we postulated that this step must require the preformation of a phosphine-ligated Ni(0) species in situ and only the four reactive phosphines are capable of reacting with the Ni(COD)₂ (COD = 1,5-cyclooctadiene) precursor to result in its formation.

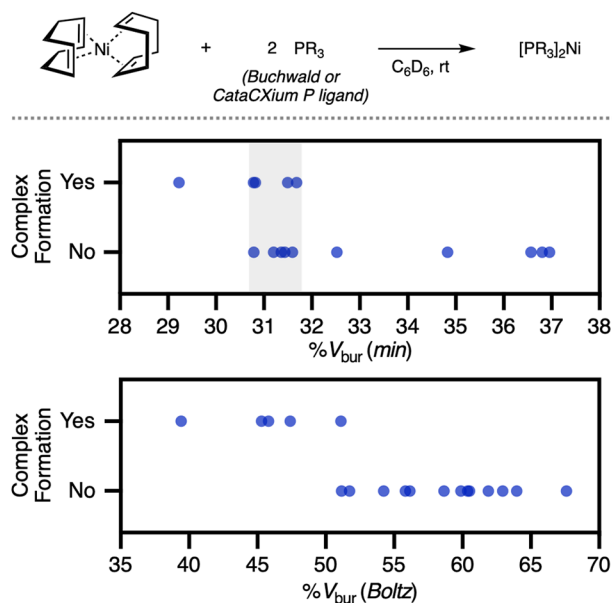
To test this hypothesis, we subjected 18 Buchwald and CataCXium P ligands to stoichiometric reactions with Ni(COD)₂. The spectra were analyzed to determine if the phosphine could form a new ligated complex (Figure 4A). In these studies, we found that only the four active Buchwald-type ligands of Reaction **I** and **Ib** displaced COD to any appreciable degree.^{43,44} None of the inactive Buchwald-type phosphines in Reaction **I**—those containing either *t*-Bu groups (e.g., JohnPhos) or significant steric bulk at the B ring *ortho* positions (e.g., SPhos, XPhos)—were found to bind. We then investigated the ability of ligand steric descriptors to rationalize COD displacement/complex formation. In alignment with the catalytic results for Reaction **I**, %*V*_{bur} (*min*) alone could not

distinguish ligands that formed complexes from those that did not. However, %*V*_{bur} (*Boltz*)—an energy-weighted representation of the ligand's average overall size—was quite successful: only ligands with %*V*_{bur} (*Boltz*) values less than 52% formed complexes under the conditions (Figure 4A).

We sought to structurally characterize a representative example of these species using single crystal X-ray diffraction (SCXRD) analysis. Despite the low conversion, we obtained single crystals of the CyJohnPhos Ni complex (co-crystallized with unreacted Ni(COD)₂) by cooling a reaction solution in pentane to −78 °C. The crystal structure of **1** revealed two CyJohnPhos ligands bound to Ni: one with a relatively low %*V*_{bur} conformation (36.8%) with κ¹-P (monodentate) binding, and the other as a high %*V*_{bur} conformation (53.4%) with κ¹-P, η²-C_{arene} (pseudobidentate) binding and evidence of substantial backbonding into the arene (Figure 4B), resulting in a formally 16 e[−] [PR₃]₂Ni(0) species.^{30,45,46} The Ni-arene interaction in **1** is significantly more pronounced than that of the analogous (CyJohnPhos)₂Pd(0) complex reported by Fink and co-workers,¹⁶ as judged by X-ray crystal structure bond metrics and distortions (see the Supporting Information for comparison of bond metrics).

To study the reactivity of **1** further, along with the analogous [PR₃]₂Ni complexes of the three other reactive ligands from Reaction **I**, we tested synthetic strategies to afford the complexes in the absence of COD or other π-accepting ligands that commonly support Ni(0) precursors.^{3,47–49} We found that the reduction of Ni(acac)₂ with AlMe₃ in the presence of 2 equiv of ligand gave **1** in good yield. This strategy was successfully applied to synthesize (CataCXium PCy)₂Ni (**2**), (CataCXium PInCy)₂Ni (**3**), and (CataCXium POMeCy)₂Ni (**4**) (Scheme 2). **2–4** were also characterized

A. Studying the ability of Buchwald ligands to displace COD from Ni(COD)₂



B. Determination of the CyJohnPhos/Ni species in solution

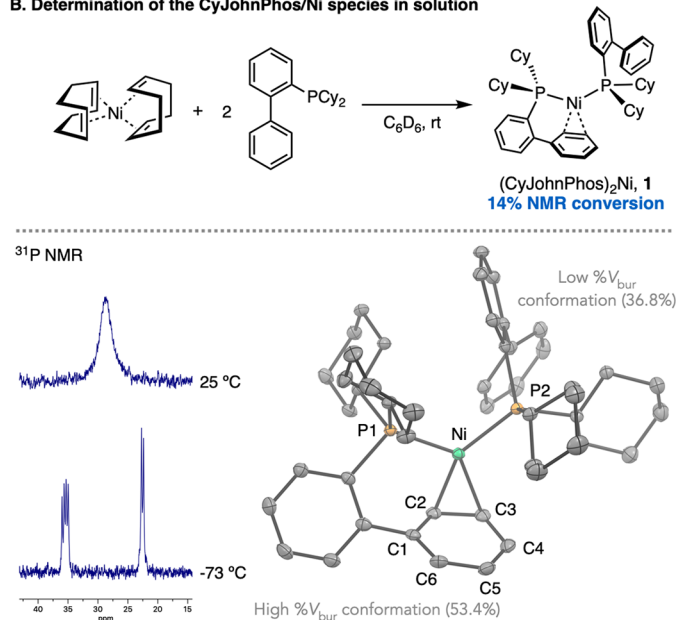
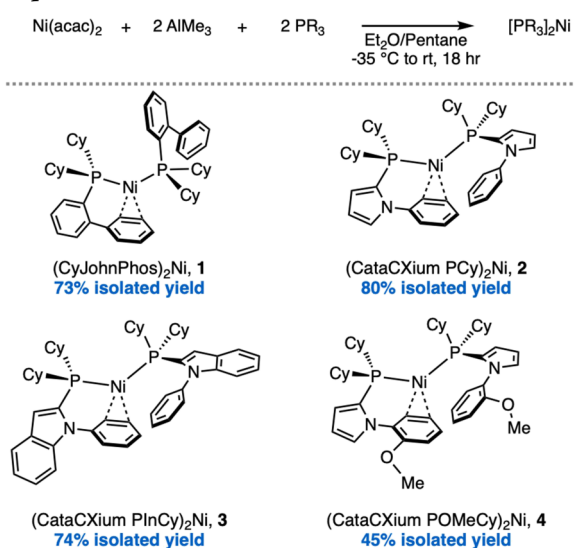


Figure 4. (A) Ligation experiments of Buchwald-type phosphines with Ni(COD)₂ (Reaction **V**). Complex formation determined by ¹H and ³¹P NMR. Shaded gray region indicates area of overlap. (B) Characterization of Ni(CyJohnPhos)₂, **1**. ³¹P{¹H} NMR of the complex at 25 °C (top) and −73 °C (bottom). Solid-state structure with thermal ellipsoids at 50% probability shown. Hydrogen atoms omitted for clarity. Selected bond distances (Å): Ni–P1: 2.1905(5); Ni–P2: 2.1887(6); Ni–C2: 1.972(1); Ni–C3: 2.075(1); C1–C2: 1.444(2); C1–C6: 1.368(2); C2–C3: 1.426(2); C3–C4: 1.436(2); C4–C5: 1.361(2); C5–C6: 1.430(2).

using SCXRD, and their structure and bonding were similar to **1** (see the [Supporting Information](#) for structural details).

Scheme 2. Synthesis and Isolation of $[\text{PR}_3]_2\text{Ni}(0)$ Complexes^a



^aX-ray structures of **2–4** can be found in the [Supporting Information](#).

Based on these structures, the % V_{bur} (*Boltz*) threshold for complex formation can be rationalized, as the ligand with $\kappa^1\text{-P}, \eta^2\text{-C}_{\text{arene}}$ (pseudobidentate) binding must not be so large that it crowds Ni's first coordination sphere to prevent the $\kappa^1\text{-P}$ (monodentate) ligand from favorably binding. Indeed, **3** was the only example of this complex class we were able to access with any *ortho*-substitution on the B ring. Furthermore, the reduction strategy did not allow us to access analogous structures with bulkier phosphines, with only decomposition or formation of unidentified/nonisolable species observed by NMR. Thus, the % V_{bur} (*Boltz*) $[\text{PR}_3]_2\text{Ni}$ complex-formation threshold observed in [Figure 4A](#) seems to extend beyond reactions with $\text{Ni}(\text{COD})_2$ and may reflect complex stability more generally.

Testing **1–4** in catalysis, we found that all four complexes were active precatalysts in Reaction I, consistent with the requirement for attaining the preligated Ni(0) species to initiate the catalytic cycle (see the [Supporting Information](#) for details). Isolation of these species also gave us the ability to study oxidative addition stoichiometrically. We anticipated that a better understanding of this step, in addition to identification of Buchwald-type ligand-bound Ni(II) species that formed after oxidative addition, would allow us to mechanistically rationalize the % V_{bur} (*min*) reactivity threshold observed across Reactions I–III.

Studying Oxidative Addition with CyJohnPhos₂Ni(0).

Using **1** as a model complex, we performed a stoichiometric oxidative addition reaction with 2 equiv of 2-chloro-5-fluorotoluene at room temperature and monitored the reaction by ³¹P and ¹⁹F NMR. A ³¹P resonance consistent with a new diamagnetic CyJohnPhos-bound Ni species was observed within minutes, and conversion of the aryl chloride was concurrently observed by ¹⁹F NMR. Unexpectedly, the new ¹⁹F resonance for the predominant species that formed (with good mass balance) matched that of 3-fluorotoluene. Minimal conversion to other species that would be consistent with aryl-

bound Ni was observed. Furthermore, after 1 h and complete conversion of **1**, >50% (relative to Ni) of the aryl chloride remained, and a substantial amount of Ni black and free phosphine was observed ([Figure 5A](#)). By ¹H NMR, a new paramagnetic species was also observed, albeit in relatively small amounts.⁵⁰

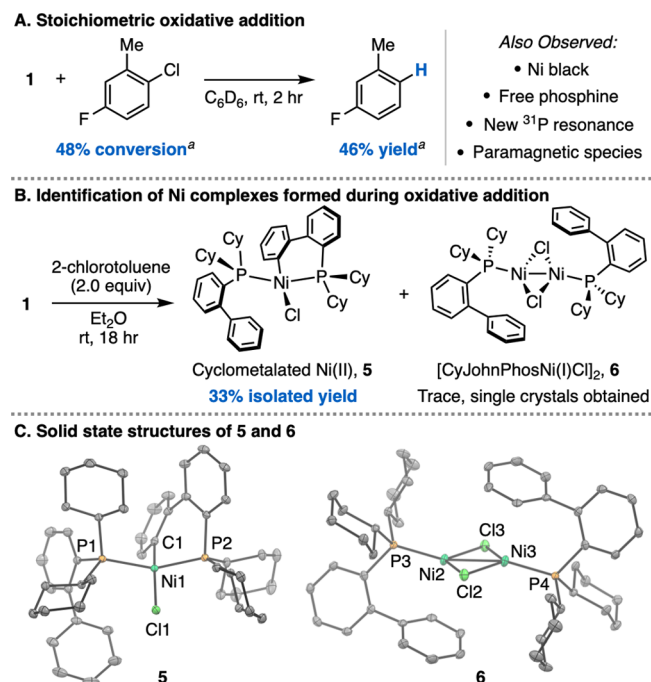
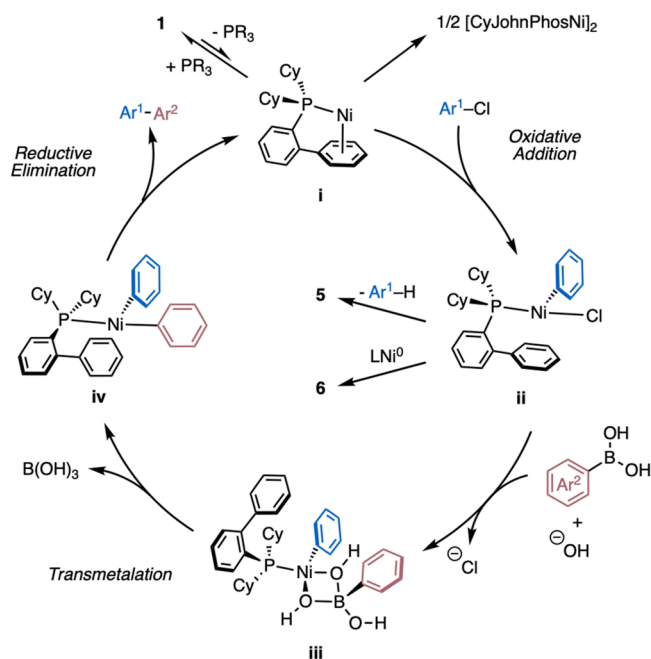


Figure 5. (A) Oxidative addition of **1** to 2-chloro-5-fluorotoluene, monitored by ¹H, ¹⁹F, and ³¹P NMR. 2.0 equiv of 2-chloro-5-fluorotoluene used relative to **1**. ^a Conversion and yield are relative to 1.0 equiv of **1** and were determined using ¹⁹F NMR using a 2-fluorobiphenyl internal standard. (B) Isolation of cyclometalated CyJohnPhos Ni(II) adduct. (C) Solid state structures of **5** and **6**, with thermal ellipsoids displayed at 50% probability and hydrogen atoms omitted for clarity. Selected bond distances (Å) for **5**: Ni–P1: 2.1863(4); Ni–P2: 2.2628(4); Ni–C1: 1.908(1); Ni–Cl1: 2.2192(3). Selected bond distances (Å) for **6**: Ni2–Ni3: 2.5530(3); Ni2–P3: 2.1749(4); Ni2–Cl2: 2.2478(3).

The effects of ligand stoichiometry on oxidative addition were then examined by conducting the reaction in the presence of 10 equiv of free CyJohnPhos. The addition of free ligand did not substantially affect the overall conversion of **1** and aryl chloride, and the same species and products were observed by NMR. This suggests that excess free ligand does not stabilize or trap reactive species to prevent decomposition to a great extent. However, the additional free ligand substantially increased the time needed to reach full conversion of **1** (and maximum conversion of the aryl chloride) compared with the reaction where no free ligand was added, implicating the intermediacy of $L_1\text{Ni}(0)$ species prior to and/or during the oxidative addition step (see the [Supporting Information](#)).

Density functional theory (DFT) studies were used to supplement our experimental findings of the oxidative addition of **1** to aryl chlorides. Given the observation that excess free ligand inhibits oxidative addition, we found that the dissociation of 1 equiv of CyJohnPhos from **1** led to an 18 e[−] $L_1\text{Ni}(0)$ species with an η^6 -arene interaction between the Ni and the CyJohnPhos B ring (intermediate **i**, [Scheme 3](#)).^{51,52} A ΔG_{dissoc} of 13.9 kcal/mol was found at the M06/def2-TZVP//

Scheme 3. Proposed Catalytic Cycle for Ni-Catalyzed SMCs with CyJohnPhos^a

^aSee the Supporting Information for the reaction free energy profile.

B3LYP-D3/6-31G(d,p) (SDD for Ni) level of theory. Following complexation of the aryl chloride to the L_1Ni species, a C–Cl bond cleavage transition state was found with an energy of 25.9 kcal/mol relative to **1** (12.0 kcal/mol relative to **i**), with η^2-C_{arene} interactions between the Ni and B ring stabilizing the otherwise unsaturated L_1Ni species. Despite the high degree of unsaturation of the resulting 14 e^- oxidative adduct **ii** (Scheme 3), no stabilizing interaction between the Ni and arene was observed in the computationally optimized structure. Dimerization of **ii** and formation of the $L_2Ni(II)$ oxidative adduct were both computed to proceed to species slightly downhill of **ii**. However, given that none of these species were consistent with the spectroscopic analysis of the resulting oxidative addition product, we postulated that **ii** must decompose in the absence of other substrates or smaller donor ligands.

To identify the new diamagnetic Ni species observed in situ by ³¹P NMR, oxidative addition of **1** to 2-chlorotoluene was then carried out on a larger scale. We isolated and crystallized the resulting air-stable species (**5**, Figure 5B) and analyzed it by SCXRD (Figure 5C). The crystal structure of **5** confirmed that the aryl from the electrophile was not bound to Ni and that one of the CyJohnPhos ligands had undergone a C–H activation and concurrent cyclonickelation, consistent with the detection of protodemetalated 3-fluorotoluene in situ (*vide supra*). This type of catalyst deactivation is well known in Pd catalysis with Buchwald ligands possessing unsubstituted B rings. However, with Ni, it is notable that this C–H activation occurs rapidly, under such mild conditions, and with a nonchelating ligand.^{53–61} Furthermore, this cyclometalation occurred significantly faster than that in the analogous CyJohnPhos/Pd system reported by Fink.¹⁶ Computationally, we were unable to locate a reasonable transition state from **ii**, the $L_2Ni(II)$ structure, or the $\mu\text{-Cl Ni(II)}$ dimer that would lead to **5**.⁶²

Despite only forming in trace amounts, we were also able to obtain single crystals of the paramagnetic species observed in situ during the oxidative addition experiments of **1** to 2-chloro-5-fluorotoluene. The solid-state structure of **6** revealed a $\mu\text{-Cl}$ bridged Ni(I) dimer species (Figure 5B), with one CyJohnPhos bound per Ni center and minimal (if any) interaction between Ni and CyJohnPhos B rings (Figure 5C).⁴⁵ The Ni–Ni distance was found to be 2.5530(3) Å, consistent with a weak Ni–Ni bond.⁶³ To the best of our knowledge, **6** represents the first structurally characterized $L_1Ni(I)$ halide dimer with a monophosphine, analogous to Sigman's dimer with NHCs.^{64–66} The ¹H NMR spectrum of the crystals matched that of the species detected in situ during the oxidative addition reactions. We were unable to isolate enough **6** to reliably perform Evans' Method measurements, but only minimal signal was detected by EPR spectroscopy (see the Supporting Information), consistent with an integer spin dimer as the predominant species in solution. Additional mechanistic studies into the formation of off-cycle species **5** and **6** and their implications in catalysis are underway.

In summary, only the smallest Buchwald-type ligands—those that possess minimal B ring substitution and alkyl groups smaller than *t*-Bu—are capable of displacing COD from Ni(COD)₂ and forming $[PR_3]_2Ni$ species. The ability to form these complexes in situ in Reaction I was required to activate the electron-rich aryl chloride and undergo oxidative addition. However, in the absence of other reaction components, the resulting coordinatively unsaturated Ni(II) complex is susceptible to decomposition and off-cycle pathways, particularly with the lack of protective B ring 2,6-substitution.^{9,10}

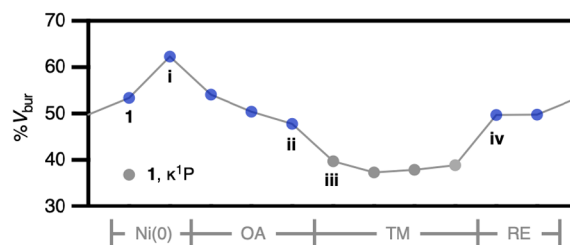
Case Study 2: Investigation of SRRs at Ni(II) in Ni-Catalyzed SMCs. While the stoichiometric oxidative addition with the aryl chloride partner alone proceeded inefficiently and ultimately led to deactivation/decomposition of the Ni catalyst, the catalytic SMC reactions proceeded with turnover numbers (TONs) greater than 30. This suggests that other components of the reaction can trap intermediate **ii**, prevent decomposition pathways, and ultimately drive the reaction to turnover. Unfortunately, we were unable to study the transmetalation step experimentally because of difficulties synthesizing the relevant CyJohnPhos-bound Ni(II) oxidative adducts containing halides (*vide supra*) or hydroxide, coupled with the highly reactive nature of boronic acid/boronate–Ni complexes. However, we were able to computationally study the elementary step, along with the remainder of the catalytic cycle (Scheme 3).⁶⁷

By DFT, the reaction of intermediate **ii** and trihydroxy-(phenyl)borate to displace chloride was found to proceed favorably (–2.4 kcal/mol from **ii**) to intermediate **iii**, a four-coordinate, 16 e^- 8-B-4 species (Scheme 3).^{67–69} The transition state of B-to-Ni transmetalation was found at 12.3 kcal/mol above **ii**, resulting in $L_1Ni(\text{aryl})_2$ intermediate **iv**, which was computed to readily undergo reductive elimination to regenerate **i** and drive the reaction forward. Additionally, a four-coordinate, 16 e^- $L_1 \mu\text{-OH}$ dimer complex with CyJohnPhos was investigated computationally.^{67,70} While it is likely an off-cycle species that must be broken up prior to transmetalation, its stability (43.3 kcal/mol lower than **ii** + [–]OH) may serve to trap **ii** and prevent cyclonickelation during catalysis.⁷¹

Re-examining the proposed SMC cycle in the context of the % V_{bur} (min) reactivity thresholds observed in Reactions I and II, we calculated the % V_{bur} values of CyJohnPhos in the DFT-

generated intermediates and transition states. The % V_{bur} values of CyJohnPhos in the intermediates prior to and after transmetalation were near or greater than 50%, consistent with the B ring fully occupying a coordination site on Ni. However, during the steps of transmetalation, the boronic acid (or OH⁻ in the case of the μ -OH dimer) occupied two of four coordination sites in the square plane, forcing the B ring to swing away from Ni, lowering the % V_{bur} of the ligand to 35–39% (Figure 6A).⁷² Thus, the mechanistic rationale most

A. % V_{bur} of CyJohnPhos during computed steps of SMC catalytic cycle



B. DFT-calculated transmetalation structures with SPhos and XPhos

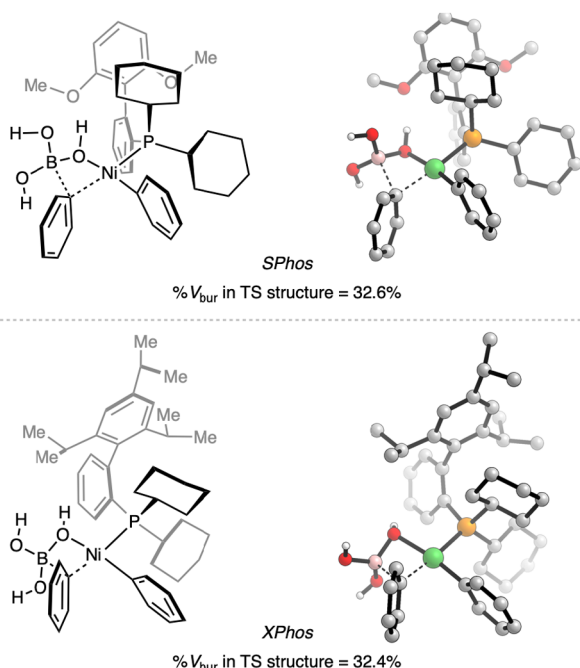


Figure 6. (A) % V_{bur} of CyJohnPhos during the DFT-optimized steps of the SMC catalytic cycle at the M06/def2-TZVP//B3LYP-D3/6-31G(d,p) [SDD] level of theory (see the Supporting Information for details). Blue dots represent conformers where the B ring occupies second coordination site, gray dots represent a conformation of CyJohnPhos where the B ring is >3.0 Å away from Ni (κ^1 -P, monodentate). (B) DFT-optimized B-to-Ni transmetalation transition state structures with SPhos and XPhos. All % V_{bur} calculations performed using SambVca 2.1.

consistent with the observed reactivity thresholds is that the ligand must be able to attain conformations in which it will occupy only one of Ni's coordination sites, allowing for both the stabilization of Ni(II) by additional σ -donor ligands and the key binding events of the substrates.

Buchwald-type ligands with B ring substitution and % V_{bur} (*min*) values less than 33% (e.g., SPhos and XPhos) were also reactive in Reaction II, despite their inability to react with Ni(COD)₂ on their own. Given the high amount of

background reactivity of Ni(COD)₂ in the absence of phosphine in this reaction and the activated, electron-deficient nature of the aryl chloride, it is likely that the electrophile reacts directly with Ni(COD)₂. The phosphine would then bind later in the catalytic cycle (i.e., at Ni(II)) to facilitate transmetalation and reductive elimination. In studying SPhos and XPhos computationally at Ni(II), their ability to adopt conformations with the substituted B ring rotated entirely behind the phosphorus lone pair/cyclohexyl rings (% V_{bur} values $\sim 32\%$) enabled favorable boronic acid binding and transmetalation (Figure 6B) with the phosphine bound.

While we were unable to obtain X-ray structures of these intermediates with Ni, this analysis and interpretation are consistent with structural evidence of SPhos and XPhos on Pd, wherein they often adopt low % V_{bur} conformations on Pd(II) with an additional σ -donor ligand bound.^{73,74} However, for Buchwald-type ligands that possess either *t*-Bu groups bound to phosphorus (e.g., JohnPhos) and/or substitution on the A ring (e.g., BrettPhos)—both modifications reflected by increased % V_{bur} (*min*) values—the inability to adopt truly monodentate structures appears to impede their successful use in Ni-catalyzed SMC reactions of aryl halides and boronic acids.

Case Study 3: Buchwald-Type Ligand Reactivity in a Ni-Catalyzed C–N Coupling. Over the past decade, significant advancements have been made in the methodology development of Ni-catalyzed C–N couplings, which are most commonly facilitated by bisphosphines.^{39,75–80} While monophosphines generally do not promote reactivity in these reactions, a screen of monophosphines in Reaction III—a C–N coupling of 4-chlorobenzotrifluoride and morpholine (Figure 3A)—revealed that several Buchwald-type ligands were uniquely capable of promoting catalytic reactivity. The reaction exhibited a similar % V_{bur} (*min*) reactivity threshold with Buchwald-type phosphines as Reaction II, although no background reactivity from Ni(COD)₂ in the absence of phosphine was observed, resulting in a much more pronounced reactivity threshold (Figure 3B). Other than Buchwald and CataCXium P ligands, only the smallest monophosphines screened (e.g., PEt₃) promoted the reaction to any appreciable degree ($<20\%$).⁸¹ This indicates that Buchwald-type ligands are privileged among monophosphines in this reaction, with CyJohnPhos as the top performer using Ni(COD)₂.

Given that the first steps of the catalytic cycle of Reaction III should be nearly identical to those of SMC Reactions I and II, we began by studying the effects of the amine on complexation following oxidative addition. Specifically, we were interested to observe if the presence of the σ -donor ligand could trap ii (Scheme 3) and form a stable 16 e⁻ complex, preventing cyclonickelation, comproportionation, and other decomposition pathways. We found that the stoichiometric oxidative addition reaction of 1 to 4-chlorobenzotrifluoride, as well as with 2-chloro-5-fluorotoluene (*vide supra*), proceeded efficiently to a new Ni complex that was spectroscopically consistent with a Ni(II) oxidative addition product containing both the phosphine and the aryl group. No evidence of off-cycle cyclonickelated species 5 or Ni(I)-Cl dimer 6 was found spectroscopically, indicating that the σ -donating morpholine was indeed capable of trapping ii, preventing decomposition (Figure 7A).

Because of the presence of excess free phosphine when starting from 1, we opted to isolate a representative morpholine-bound Ni complex from Ni(COD)₂, 2 equiv 4-

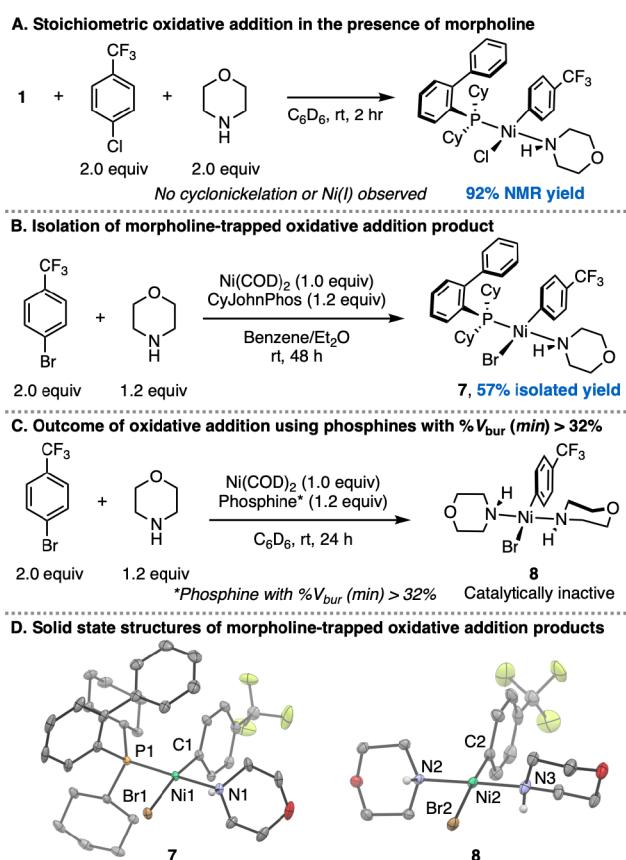


Figure 7. (A) Oxidative addition of **1** to 4-chlorobenzotrifluoride in the presence of morpholine. Yield determined by ^{19}F NMR with a 2-fluorobiphenyl internal standard. (B) Isolation of the morpholine-trapped oxidative addition product with CyJohnPhos. (C) Observation of the off-cycle bis-morpholine bound oxidative addition product. See the Supporting Information for isolation conditions of the authentic product. (D) Solid-state structures of **7** and **8**. Hydrogens bound to carbon omitted for clarity. Selected bond distances (Å) for **7**: Ni1–P1: 2.1906(5); Ni1–N1: 1.993(1); Ni–C1: 1.881(1); Ni–Br1: 2.4119(5). Selected bond distances (Å) for **8**: Ni2–N2: 1.947(1); Ni2–N3: 1.949(2); Ni2–C2: 1.881(2); Ni2–Br2: 2.4204(4).

boromobenzotrifluoride, and a slight excess of both CyJohnPhos and morpholine. This reaction successfully afforded **7** (Figure 7B) in 57% yield. We were able to characterize **7** by SCXRD, structurally confirming that morpholine had trapped the oxidative adduct as a stable four-coordinate $16 e^-$ complex,^{73,82} preventing the cyclonickelation pathway. Similar to the DFT-optimized structures during SMC transmetalation, the B ring of CyJohnPhos in **7** had rotated out of the first coordination sphere almost entirely and adopted a conformation with a relatively low % V_{bur} of 37.3%. A favorable C–H $\cdots \pi$ interaction between the Ni-bound aryl and the B Ring of CyJohnPhos stabilized this slightly higher % V_{bur} conformation (see the Supporting Information for details).

Access to **7** gave us a unique opportunity to stoichiometrically observe and study N–H deprotonation and subsequent C–N reductive elimination from an on-cycle amine-bound Ni complex.^{83,84} We found that combining **7** with a slight excess of NaOt-Bu in a stoichiometric NMR study under inert atmosphere gave C–N coupled product in 89% NMR yield (Figure 8A), which had reached maximum conversion by the time the spectrum was taken (<5 min). This indicates that the

deprotonation and reductive elimination steps occurred rapidly, even at room temperature, suggesting that the C–N bond-forming transition state barrier from the deprotonated complex is low. We also tested **7** as precatalyst in Reaction III. We found that it was a reactive precatalyst in the reaction, with about 30 turnovers observed within minutes, even at room temperature (Figure 8B).

DFT studies showed that the reductive elimination barrier from the Ni amido species (intermediate GS28, Figure 8C) was 13.3 kcal/mol, consistent with the experimental observation of rapid reductive elimination at room temperature in the presence of a base. The B ring of the arene rotated back to block the fourth coordination site during reductive elimination, ultimately forcing the coupling partners *cis* on Ni's square plane. The Ni–C distances between Ni and the B ring were all >2.75 Å for GS28 and TS10 (Figure 8C), indicative of highly reactive $14 e^-$ intermediates. Overall, the full free energy profile for the C–N coupling reaction with CyJohnPhos (Figure 8C) demonstrates the very low transition state barriers for all steps. The importance of Buchwald-type ligand hemilability in this catalytic cycle is also evident, as the B ring stabilizes Ni(0), but enforces coordinatively unsaturated, highly reactive Ni(II) species. To this end, upon comparing the computed C–N reductive elimination barriers of Buchwald ligands and chelating bisphosphines, we found that CyJohnPhos and XPhos had notably lower ΔG^\ddagger values (13.3 and 10.7 kcal/mol, respectively) than bisphosphine dppf and PhPAD-DalPhos (15.8 and 14.3 kcal/mol, respectively).

Attempts to isolate complexes analogous to **7** with SPhos and XPhos were unsuccessful despite their reactivity in Reaction III. For both, in situ NMR studies of the stoichiometric oxidative addition in the presence of morpholine did indicate that a new phosphine-ligated Ni(II) complex formed, albeit in low yields (see the Supporting Information). By DFT, these complexes likely had phosphines bound with % V_{bur} values close to 32%, allowing for the fourth coordination site to be accessed by the amine. While these phosphine-ligated complexes are attainable in solution and in catalysis, the only species that we could isolate and crystallize was **8** (Figure 7C).⁸⁵ This catalytically inactive bis-morpholine ligated complex was the exclusive oxidative addition product observed with Buchwald-type phosphines possessing % V_{bur} (min) values >32%. In addition to allowing access to the additional coordination site for amine binding, the % V_{bur} (min) reactivity threshold in Reaction III could also be reflective of congested transition states during substrate deprotonation and/or ligand substitutions with *tert*-butoxide, where Ni's first coordination sphere may be required to be unencumbered by the phosphine.

To summarize our findings from this case study, σ -donating amine substrates can bind to and stabilize $L_1\text{Ni}$ oxidative adducts with Buchwald-type ligands. However, the B ring of the phosphine must rotate out of the first coordination sphere in order for the coordination site to be accessed by the amine, which requires no A ring substitution and alkyl groups smaller than *t*-Bu. The resulting $16 e^-$ complexes, such as **7**, rapidly undergo deprotonation and C–N bond-forming reductive elimination at room temperature in the presence of a base and are promising precatalysts for this reaction class.

Case Study 4: Structural Studies of Ni(0) Aldehyde Complexes with Buchwald-Type Ligands. In the final case study, we investigated Reaction IV, which was reported by our laboratory in 2011. In the original study, it was found that the use of Buchwald-type ligands was necessary to enable high

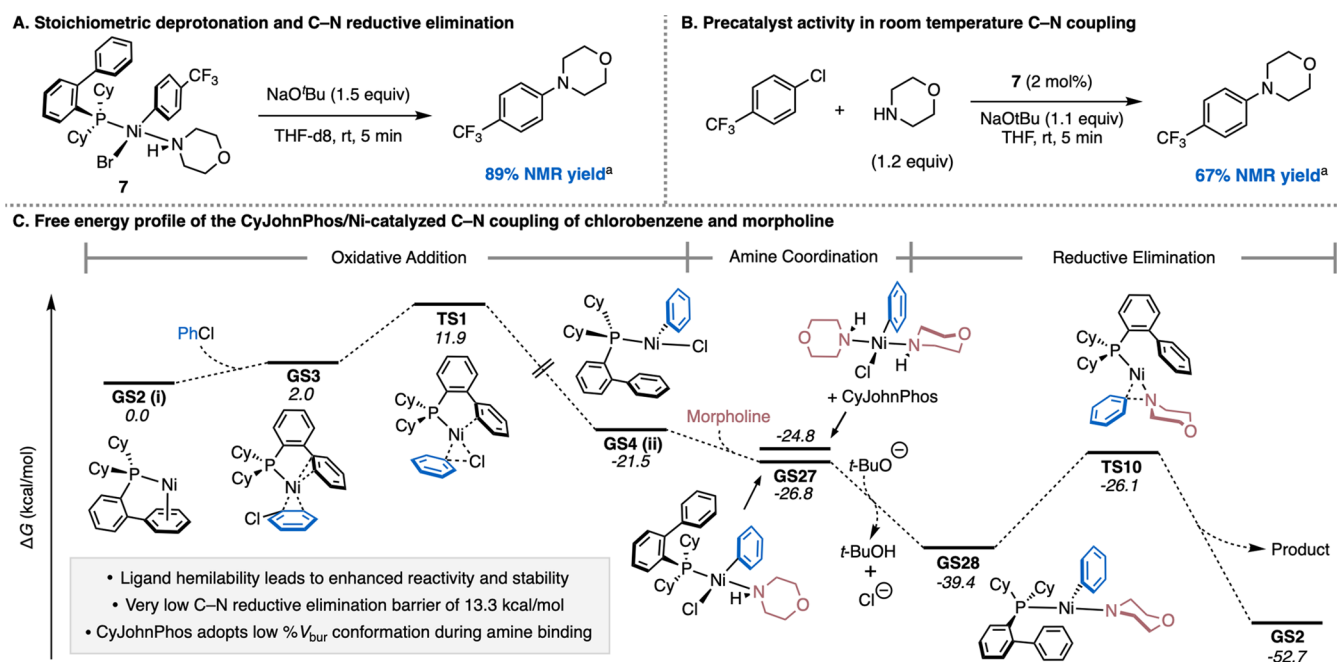
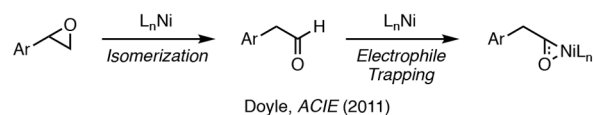


Figure 8. (A) Stoichiometric reductive elimination studies with **7**. (B) Room temperature precatalyst reactivity studies with **7** in Reaction III. ^a NMR (¹⁹F) yields determined relative to a 2-fluorobiphenyl internal standard. (C) Free energy profile of the C–N coupling reaction catalyzed by **7**. DFT calculations performed at the M06/def2-TZVP//B3LYP-D3/6-31G(d,p) [SDD for Ni] level of theory with a SMD solvation model (THF).

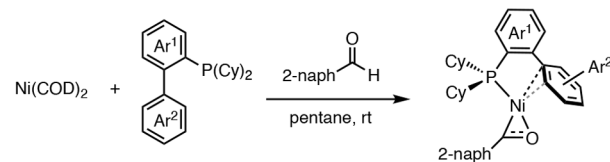
reactivity and that bulky BrettPhos was the highest performing example tested.¹⁹ Re-evaluating the ligands screened in the reaction, no % V_{bur} (*min*) reactivity threshold was observed, and Buchwald-type ligands of all steric profiles were active above background reactivity (Figure 3B). Unlike the previous case studies, this transformation is an example of a cross-coupling reaction of an unconventional electrophile, where the standard elementary steps of Csp^2 –X activation/oxidative addition do not necessarily apply. Specifically, the mechanism of styrene oxide activation was proposed by Nielsen and Doyle to first proceed through isomerization, generating phenylacetaldehyde in situ, followed by Ni complexation and arylation (Figure 9A); notably, the reaction was found to proceed directly from phenylacetaldehyde, although from a methodological standpoint, styrene oxide was the preferred electrophile.¹⁹

In our 2011 report, an off-cycle intermediate of the isomerization pathway was isolated, with Ni(II) bound to the 4-position of the dearomatized B ring of BrettPhos. To the best of our knowledge, this represented the only other structurally characterized Ni complex with a Buchwald ligand before this study. However, subsequent trapping of the aldehyde was not investigated, and it remained unclear how the ligand interacted with Ni structurally during this step. Recently, we used 4-fluorobenzaldehyde to spectroscopically determine the ligation state of Ni with various phosphines, including Buchwald-type phosphines. The stability of the complexes in solution suggested that benzaldehyde derivatives may provide a stable trap for both L_2Ni and L_1Ni species, allowing for the study and isolation of L_1Ni (aldehyde) complexes with Buchwald ligands.²⁶ Indeed, we found that most Buchwald-type ligands, regardless of their % V_{bur} values, could form L_1Ni (4-fluorobenzaldehyde) complexes from $Ni(COD)_2$ (Figure 10) as detected by NMR. The two exceptions were (*t*-Bu)BrettPhos and (*t*-Bu)XPhos, whose considerable steric bulk prevented ligation altogether. However, certain Buchwald ligands with *t*-Bu groups bound to

A. Proposed mechanism for styrene oxide activation in Reaction IV



B. Synthesis of L_1Ni (2-naphthaldehyde) complexes with Buchwald Ligands



C. X-ray structures of L_1Ni (2-naphthaldehyde) complexes

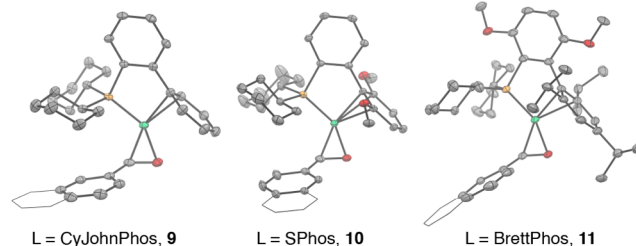


Figure 9. (A) Activation of styrene oxide in Reaction IV proposed by Nielsen and Doyle. (B) Synthesis of L_1Ni (2-naphthaldehyde) complexes with Buchwald ligands from $Ni(COD)_2$. (C) X-ray crystal structures of L_1Ni (2-naphthaldehyde) complexes with CyJohnPhos, SPhos, and BrettPhos. Thermal ellipsoids displayed at 50% probability for **9** and **10**, and 30% probability for **11**. Hydrogen atoms omitted for clarity.

phosphorus that had no B ring substitution (e.g., JohnPhos) or mono B ring substitution (e.g., (*t*-Bu)MePhos) could form complexes in the experiments, as determined by NMR.

Given that no % V_{bur} (*min*) steric threshold was observed in Reaction IV or in the spectroscopic experiments with 4-fluorobenzaldehyde, we hypothesized that the ligands would

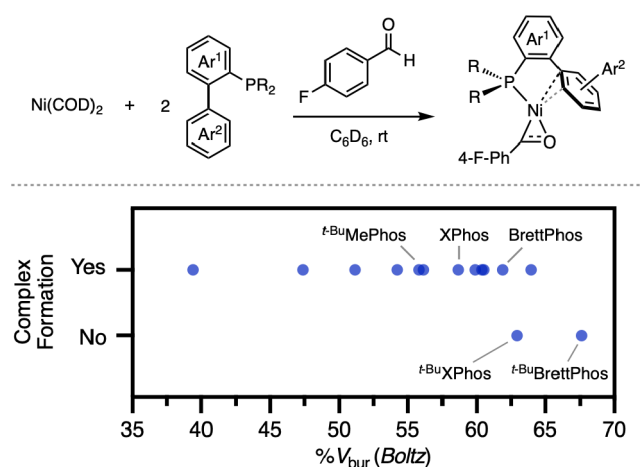


Figure 10. NMR studies with 4-F-benzaldehyde (Reaction VI). Complex formation determined by ^1H , ^{19}F , and ^{31}P NMR.

adopt high $\%V_{\text{bur}}$ conformations (with the B ring fully occupying a coordination site) when bound to Ni-aldehyde complexes. For ease of synthesis and crystallization, 2-naphthaldehyde was chosen to isolate complexes bearing a selection of phosphines: CyJohnPhos, SPhos, and BrettPhos (9–11, Figure 9C). For each of the three complexes, the X-ray structure revealed that the B ring of the phosphine was indeed fully occupying a coordination site on Ni, with ligand $\%V_{\text{bur}}$ values of 53.2, 56.0, and 60.7% for 9, 10, and 11, respectively. Thus, for these complexes, the phosphine occupies more than 50% of Ni's first coordination sphere/two of four coordination sites, preventing additional ligand or substrate equivalents from binding. While less π -basic than the Ni centers of 1–4, stabilizing $\eta^2\text{-C}_{\text{arene}}$ interactions ($\eta^1\text{-C}_{\text{arene}}$ in the case of 10 with SPhos) are still present to result in 16 e^- Ni(0) species, with indications of backbonding into the B ring evident through C–C bond elongations and distortions (see the Supporting Information).

We found that the BrettPhos complex 11 was an active precatalyst in Reaction IV, which suggests that this species is relevant in catalysis and supports the mechanistic proposal of Nielsen and Doyle. While the exact mechanism of aldehyde arylation from the boronic acid coupling partner is still unclear, the observation that the most active ligands were those that enforce occupation of two coordination sites suggests that the 1,2 arylation pathway may not proceed through traditional B-to-Ni transmetalation (*vide supra*).⁸⁶

Reactivity of Buchwald Ligands with Ni(stb)₃ Precursors. The observed stability of 9–11 with a monodentate π -accepting ligand (i.e., 2-naphthaldehyde), combined with the challenges associated with the Buchwald-type ligand displacement of bidentate COD from Ni(COD)₂, led us to examine the structure and reactivity of Buchwald ligand-bound Ni(0) complexes derived from Ni(stb)₃.^{47,48} The Cornell laboratory has recently shown that these 16 e^- Ni(0) complexes are versatile catalytic precursors and are even air-stable as solids, particularly when the stilbene ligands are decorated with bulky groups at the *para* positions.^{47,48}

We selected six Buchwald ligands (CyJohnPhos, SPhos, XPhos, DavePhos, JohnPhos, and BrettPhos) and studied their stoichiometric reactivity with Ni(stb)₃ using a 1:1 L₁Ni(stb) complex. Unlike with Ni(COD)₂, high conversion to an L₁Ni(stb) complex was observed using *in situ* ^1H and ^{31}P NMR spectroscopy for all ligands but BrettPhos (less than 10%

conversion to LNi(stb), Figure 11A). Similar results were observed for the commercially available and more air-stable

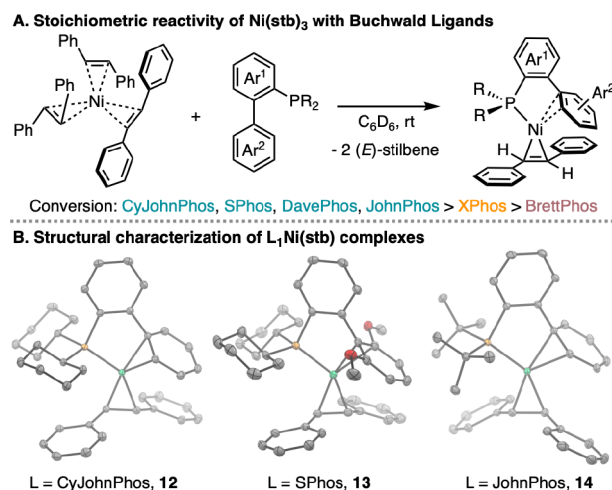


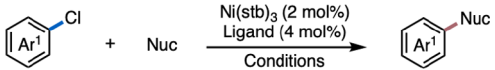
Figure 11. (A) Stoichiometric reaction of Ni(stb)₃ with Buchwald ligands, analyzed by ^1H and ^{31}P NMR spectroscopy. CyJohnPhos, SPhos, DavePhos, and JohnPhos reacted with conversions greater than 80% (green), XPhos 66% (orange), and BrettPhos 20% (red) as determined by $^{31}\text{P}\{^1\text{H}\}$ NMR. (B) Solid-state structures of L₁Ni(stb) complexes with L = CyJohnPhos (12), SPhos (13), and JohnPhos (14). Thermal ellipsoids displayed at 50% probability and hydrogen atoms omitted for clarity.

Ni(*t*-Bu-stb)₃, although the conversions were generally slightly lower, likely due to the increased stability of the precursor afforded by the 4-*t*-Bu groups.⁴⁸

We obtained SCXRD characterization of the CyJohnPhos, SPhos, and JohnPhos L₁Ni(stb) complexes, confirming the pseudobidentate binding of the phosphines to Ni with strong η^2 -arene interactions observed between Ni(0) and the phosphine B ring in each case (12–14, Figure 11B). As judged by bond metrics from the X-ray crystal structures, the η^2 -arene interaction in (CyJohnPhos)Ni(stb) (12) was stronger than that of (CyJohnPhos)Ni(2-naphthaldehyde) (9) but weaker than that of (CyJohnPhos)₂Ni (1) (see the Supporting Information for compiled table), which is rationalized well by the σ -donor/ π -acceptor abilities of the second ligand bound.

The catalytic competency of these complexes was tested on Reactions I, II, and III (Table 1). Overall, we found that the reactivity trends and active/inactive ligands in the threshold analysis were similar between the Ni(stb)₃ precursors and Ni(COD)₂. Consistent with the threshold analysis, the two ligands with $\%V_{\text{bur}}$ (*min*) values >32% (JohnPhos and BrettPhos) that were tested with Ni(stb)₃ precursors gave trace products, despite JohnPhos forming a ligated complex *in situ* with high conversions. While BrettPhos did not form an L₁Ni(stb) complex efficiently, the ligated (BrettPhos)Ni(2-naphthaldehyde) complex (11) was tested in Reactions I–III as a precatalyst, also only yielding trace products. Overall, these data indicate that generating a ligated precatalyst *in situ* is necessary but not sufficient to give catalytic turnover, consistent with the $\%V_{\text{bur}}$ (*min*) threshold analysis (*vide supra*).

With regard to active Buchwald ligands with Ni(stb)₃ precursors (those with relatively low $\%V_{\text{bur}}$ (*min*) values), CyJohnPhos was generally the best overall in the SMC reactions (Table 1). Furthermore, in a head-to-head

Table 1. Catalytic Reactivity Studies with Ni(stb)₃ as a Precursor^a


Ligand	Reaction I	Reaction II	Reaction III
dppf ^b	2% (16%)	1% (16%)	16% (83%)
CyJohnPhos	45% (67%)	49% (89%)	74% (68%)
CyJohnPhos ^c	82% (94%)	87% (98%)	72% (56%)
XPhos	3% (6%)	56% (49%)	92% (12%)
JohnPhos	1% (5%)	11% (19%)	1% (0%)

^aUnless otherwise noted, reaction conditions were the same as in Figure 3A (see Supporting Information for details). Yields in parentheses are with Ni(COD)₂ under otherwise same reaction conditions. ^b2 mol % dppf used. ^c2 mol % CyJohnPhos used, and the reactions were run for 2.5, 18, and 18 h for Reaction I, II, and III, respectively.

comparison with dppf, one of the most widely utilized biphosphines for Suzuki couplings and C–N couplings of secondary amines, CyJohnPhos performed significantly better under the reaction conditions with the air-stable Ni(stb)₃ precatalysts. Ligands with *ortho*-substitution still only gave trace products in Reaction I with the electron-rich 4-chloroanisole electrophile. However, for Reactions II and III with 4-chlorobenzotrifluoride, XPhos performed comparably to CyJohnPhos, significantly better with the Ni(stb)₃ precursors than Ni(COD)₂. Indeed, an 80% improvement in yield was observed for XPhos with Ni(stb)₃ compared with Ni(COD)₂ in Reaction III, where it outperformed both CyJohnPhos and dppf under the reaction conditions. These results demonstrate the importance of precatalyst design and utilization with Buchwald ligands in Ni catalysis, which with further development, should unlock the full potential of the ligand class in Ni catalyzed cross-coupling.

SUMMARY AND CONCLUSIONS

Using %V_{bur} threshold analysis alongside mechanistic organometallic investigations, we have elucidated the structure–reactivity relationships of Buchwald-type ligands in four representative Ni-catalyzed cross-coupling reactions. A summary of our findings related to the bonding, speciation, and SRRs of Buchwald-type ligands at Ni(0) and Ni(II) is below.

Ni(0):

- π -basic Ni(0) readily forms stabilizing η^2 -arene interactions with the B ring of Buchwald-type ligands.
- Ligands that possess minimal B ring substitution and alkyl groups smaller than *t*-Bu—reflected by both relatively low %V_{bur} (*min*) and %V_{bur} (*Boltz*) values—can form [PR₃]₂Ni complexes in situ from Ni(COD)₂. These complexes can undergo oxidative addition to aryl halide electrophiles.
- In these 16 e[−] complexes, one of the two phosphines adopts a high %V_{bur} conformation with pseudobidentate (κ^1 -P, η^2 -C_{arene}) binding, and the other adopts a low %V_{bur} conformation with monodentate (κ^1 -P) binding. Because of this arrangement, the ligands must be small enough to not overcrowd the complex.
- In the presence of π -accepting substrates like aldehydes that can react with Ni(COD)₂ on their own, most Buchwald-type ligands, including those that have B ring substitution and/or *t*-Bu groups, readily bind to form

L₁Ni(substrate) complexes. Similarly, Buchwald-type ligands can form L₁Ni(stb) complexes upon reaction with commercially available, air-stable Ni(stb)₃ precursors, which can serve as precatalysts.

- In these scenarios, the ligand adopts a high %V_{bur} conformation, with stabilizing η^2 -C_{arene} interactions observed between the π -basic Ni center and the B ring, resulting in 16 e[−] Ni(0). No %V_{bur} (*min*) steric threshold is observed in complex formation. However, ligands that have both 2,6-substitution on their B ring and *t*-Bu alkyl groups are too bulky to form stable complexes.

Ni(II):

- For less π -basic Ni(II), stabilizing interactions between the Ni and B ring are weak or nonexistent, thus making pseudobidentate binding insufficient to stabilize coordinatively unsaturated oxidative addition complexes.
- A σ -donating substrate must bind to the L₁Ni(II) oxidative adduct to both stabilize the otherwise 14 e[−] complex and to facilitate catalytic turnover. In the absence of these σ -donors, or if the steric profile of the phosphine prevents their binding, decomposition to Ni(I) or cyclonickelation occurs.
- The B ring of the phosphine must rotate out of the first coordination sphere to enable substrate binding. Buchwald-type phosphines with alkyl groups smaller than *t*-Bu and no A ring substitution—reflected by relatively low %V_{bur} (*min*) values—are required to enable conformations where the ligand only occupies one of four coordination sites of Ni's square plane.

In the context of the catalytic reactions studied, ligands with minimal substitution, such as CyJohnPhos and CataCXium PCy, were the most effective Buchwald-type phosphines at promoting cross-coupling of aryl halides. The ability of these ligands to readily adopt both high and low %V_{bur} conformations gives rise to hemilability (pseudobidentate at Ni(0) and monodentate at Ni(II)), which appears to be desirable in these Csp²–Csp² and Csp²–N bond-forming reactions. For reactions of unconventional cross-coupling electrophiles that involve π -complexes, larger, less conformationally flexible ligands like BrettPhos are viable candidates to promote a successful transformation.

We anticipate that the %V_{bur} classification analysis and SRR principles presented in this work will be useful in the prediction of new stoichiometric and catalytic reactivity of Buchwald-type ligands with Ni and that the threshold workflow can be readily applied to Pd catalysis where the ligand class is ubiquitous. In this light, the study should serve as a guide to chemists who wish to access well-defined organonickel complexes with Buchwald-type ligands, the further employment of the ligand class in catalysis, as well as in the design of new ligands and precatalysts for Ni. Additionally, we expect that access to well-defined Buchwald-type ligand-bound Ni precursors will enable studies into the many other manifolds of Ni catalysis yet to be explored with the ligand class. Additional mechanistic organometallic studies of the Buchwald-type ligand class with Ni, as well as their applications in catalysis, are underway in our laboratory.

■ ASSOCIATED CONTENT

SI Supporting Information

The Supporting Information is available free of charge at <https://pubs.acs.org/doi/10.1021/jacs.2c09840>.

Experimental procedures; experimental data; and characterization and spectral data for new compounds (PDF)

XYZ coordinates for DFT-computed structures (ZIP)

Accession Codes

CCDC 2077073, 2077074, 2077075, 2077076, 2077077, 2077078, 2077079, 2077083, 2077084, 2079498, 2156651, 2156652, 2156653, 2156654, 2181563, 2181564, and 2202070 contain the supplementary crystallographic data for this paper. These data can be obtained free of charge via www.ccdc.cam.ac.uk/data_request/cif, or by emailing data_request@ccdc.cam.ac.uk, or by contacting The Cambridge Crystallographic Data Centre, 12 Union Road, Cambridge CB2 1EZ, UK; fax: +44 1223 336033.

■ AUTHOR INFORMATION

Corresponding Author

Abigail G. Doyle – Department of Chemistry, Princeton University, Princeton, New Jersey 08544, United States; Department of Chemistry and Biochemistry, University of California Los Angeles, Los Angeles, California 90095, United States; orcid.org/0000-0002-6641-0833; Email: agdoyle@chem.ucla.edu

Authors

Samuel H. Newman-Stonebraker – Department of Chemistry, Princeton University, Princeton, New Jersey 08544, United States; Department of Chemistry and Biochemistry, University of California Los Angeles, Los Angeles, California 90095, United States

Jason Y. Wang – Department of Chemistry, Princeton University, Princeton, New Jersey 08544, United States; Department of Chemistry and Biochemistry, University of California Los Angeles, Los Angeles, California 90095, United States; orcid.org/0000-0001-5826-2554

Philip D. Jeffrey – Department of Molecular Biology, Princeton University, Princeton, New Jersey 08544, United States

Complete contact information is available at: <https://pubs.acs.org/doi/10.1021/jacs.2c09840>

Notes

The authors declare no competing financial interest.

■ ACKNOWLEDGMENTS

We thank Ken Conover and Dr. Ta-Chung Ong for assistance with low temperature NMR experiments, Dr. Saeed Khan for assistance with X-ray structure determination, and Dr. Paul Oyala for assistance with EPR measurements. We also thank Judah Raab, Julia Borowski, Ellyn Peters, and Prof. Matthew Sigman for helpful discussions. Financial support for this work was provided by the NIGMS (R35 GM126986).

■ REFERENCES

(1) Johansson Seechurn, C. C. C.; Kitching, M. O.; Colacot, T. J.; Snieckus, V. Palladium-Catalyzed Cross-Coupling: A Historical Contextual Perspective to the 2010 Nobel Prize. *Angew. Chem., Int. Ed.* **2012**, *51*, 5062–5085.

(2) Brown, D. G.; Boström, J. Analysis of Past and Present Synthetic Methodologies on Medicinal Chemistry: Where Have All the New Reactions Gone? *J. Med. Chem.* **2016**, *59*, 4443–4458.

(3) Hazari, N.; Melvin, P. R.; Beromi, M. M. Well-Defined Nickel and Palladium Precatalysts for Cross-Coupling. *Nat. Rev. Chem.* **2017**, *1*, No. 0025.

(4) Ruiz-Castillo, P.; Buchwald, S. L. Applications of Palladium-Catalyzed C–N Cross-Coupling Reactions. *Chem. Rev.* **2016**, *116*, 12564–12649.

(5) Surry, D. S.; Buchwald, S. L. Dialkylbiaryl Phosphines in Pd-Catalyzed Amination: A User's Guide. *Chem. Sci.* **2011**, *2*, 27–50.

(6) Martin, R.; Buchwald, S. L. Palladium-Catalyzed Suzuki–Miyaura Cross-Coupling Reactions Employing Dialkylbiaryl Phosphine Ligands. *Acc. Chem. Res.* **2008**, *41*, 1461–1473.

(7) Zapf, A.; Jackstell, R.; Rataboul, F.; Riermeier, T.; Monsees, A.; Fuhrmann, C.; Shaikh, N.; Dingerdissen, U.; Beller, M. Practical Synthesis of New and Highly Efficient Ligands for the Suzuki Reaction of Aryl Chlorides. *Chem. Commun.* **2004**, 38–39.

(8) Rataboul, F.; Zapf, A.; Jackstell, R.; Harkal, S.; Riermeier, T.; Monsees, A.; Dingerdissen, U.; Beller, M. New Ligands for a General Palladium-Catalyzed Amination of Aryl and Heteroaryl Chlorides. *Chem. – Eur. J.* **2004**, *10*, 2983–2990.

(9) Strieter, E. R.; Blackmond, D. G.; Buchwald, S. L. Insights into the Origin of High Activity and Stability of Catalysts Derived from Bulky, Electron-Rich Monophosphinobiaryl Ligands in the Pd-Catalyzed C–N Bond Formation. *J. Am. Chem. Soc.* **2003**, *125*, 13978–13980.

(10) Strieter, E. R.; Buchwald, S. L. Evidence for the Formation and Structure of Palladacycles during Pd-Catalyzed C–N Bond Formation with Catalysts Derived from Bulky Monophosphinobiaryl Ligands. *Angew. Chem., Int. Ed.* **2006**, *45*, 925–928.

(11) Barder, T. E.; Walker, S. D.; Martinelli, J. R.; Buchwald, S. L. Catalysts for Suzuki–Miyaura Coupling Processes: Scope and Studies of the Effect of Ligand Structure. *J. Am. Chem. Soc.* **2005**, *127*, 4685–4696.

(12) Barder, T. E.; Biscoe, M. R.; Buchwald, S. L. Structural Insights into Active Catalyst Structures and Oxidative Addition to (Biaryl)-Phosphine–Palladium Complexes via Density Functional Theory and Experimental Studies. *Organometallics* **2007**, *26*, 2183–2192.

(13) Ikawa, T.; Barder, T. E.; Biscoe, M. R.; Buchwald, S. L. Pd-Catalyzed Amidations of Aryl Chlorides Using Monodentate Biaryl Phosphine Ligands: A Kinetic, Computational, and Synthetic Investigation. *J. Am. Chem. Soc.* **2007**, *129*, 13001–13007.

(14) Throughout the manuscript, monoligated (L_1) is defined as a single monophosphine ligand bound to the metal center and bisligated (L_2) is defined as two monophosphine ligands bound to the metal.

(15) Yin, J.; Rainka, M. P.; Zhang, X.-X.; Buchwald, S. L. A Highly Active Suzuki Catalyst for the Synthesis of Sterically Hindered Biaryls: Novel Ligand Coordination. *J. Am. Chem. Soc.* **2002**, *124*, 1162–1163.

(16) Reid, S. M.; Boyle, R. C.; Mague, J. T.; Fink, M. J. A Dicoordinate Palladium(0) Complex with an Unusual Intramolecular η^1 -Arene Coordination. *J. Am. Chem. Soc.* **2003**, *125*, 7816–7817.

(17) Biscoe, M. R.; Fors, B. P.; Buchwald, S. L. A New Class of Easily Activated Palladium Precatalysts for Facile C–N Cross-Coupling Reactions and the Low Temperature Oxidative Addition of Aryl Chlorides. *J. Am. Chem. Soc.* **2008**, *130*, 6686–6687.

(18) Yada, A.; Yukawa, T.; Nakao, Y.; Hiyama, T. Nickel/ $AlMe_2Cl$ -Catalyzed Carbocyanation of Alkynes Using Arylacetonitriles. *Chem. Commun.* **2009**, 3931–3933.

(19) Nielsen, D. K.; Doyle, A. G. Nickel-Catalyzed Cross-Coupling of Styrenyl Epoxides with Boronic Acids. *Angew. Chem., Int. Ed.* **2011**, *50*, 6056–6059.

(20) Zhou, Q.; Cobb, K. M.; Tan, T.; Watson, M. P. Stereospecific Cross Couplings To Set Benzylic, All-Carbon Quaternary Stereocenters in High Enantiopurity. *J. Am. Chem. Soc.* **2016**, *138*, 12057–12060.

(21) Ariki, Z. T.; Maekawa, Y.; Nambo, M.; Cruden, C. M. Preparation of Quaternary Centers via Nickel-Catalyzed Suzuki–

- Miyaura Cross-Coupling of Tertiary Sulfoxes. *J. Am. Chem. Soc.* **2018**, *140*, 78–81.
- (22) Coombs, J. R.; Green, R. A.; Roberts, F.; Simmons, E. M.; Stevens, J. M.; Wisniewski, S. R. Advances in Base-Metal Catalysis: Development of a Screening Platform for Nickel-Catalyzed Borylations of Aryl (Pseudo)Halides with $B_2(OH)_4$. *Organometallics* **2019**, *38*, 157–166.
- (23) Munteanu, C.; Spiller, T. E.; Qiu, J.; DelMonte, A. J.; Wisniewski, S. R.; Simmons, E. M.; Frantz, D. E. Pd- and Ni-Based Systems for the Catalytic Borylation of Aryl (Pseudo)Halides with $B_2(OH)_4$. *J. Org. Chem.* **2020**, *85*, 10334–10349.
- (24) Koeritz, M. T.; Burgett, R. W.; Kadam, A. A.; Stanley, L. M. Ni-Catalyzed Intermolecular Carboacylation of Internal Alkynes via Amide C–N Bond Activation. *Org. Lett.* **2020**, *22*, 5731–5736.
- (25) Sabater, S.; Menche, M.; Ghosh, T.; Krieg, S.; Rück, K. S. L.; Paciello, R.; Schäfer, A.; Comba, P.; Hashmi, A. S. K.; Schaub, T. Mechanistic Investigation of the Nickel-Catalyzed Carbonylation of Alcohols. *Organometallics* **2020**, *39*, 870–880.
- (26) Newman-Stonebraker, S. H.; Smith, S. R.; Borowski, J. E.; Peters, E.; Gensch, T.; Johnson, H. C.; Sigman, M. S.; Doyle, A. G. Univariate Classification of Phosphine Ligation State and Reactivity in Cross-Coupling Catalysis. *Science* **2021**, *374*, 301–308.
- (27) Ponce-de-León, J.; Gioria, E.; Martínez-Illarduya, J. M.; Espinet, P. Ranking Ligands by Their Ability to Ease $(C_6F_5)_2Ni^{II}L \rightarrow Ni^0L + (C_6F_5)_2$ Coupling versus Hydrolysis: Outstanding Activity of PEWO Ligands. *Inorg. Chem.* **2020**, *59*, 18287–18294.
- (28) Jacobs, E.; Keaveney, S. T. Experimental and Computational Studies Towards Chemoselective C–F over C–Cl Functionalisation: Reversible Oxidative Addition Is the Key. *ChemCatChem* **2021**, *13*, 637–645.
- (29) Marín, M.; Moreno, J. J.; Navarro-Gilabert, C.; Álvarez, E.; Maya, C.; Peloso, R.; Nicasio, M. C.; Carmona, E. Synthesis, Structure and Nickel Carbonyl Complexes of Dialkylterphenyl Phosphines. *Chem. – Eur. J.* **2019**, *25*, 260–272.
- (30) Martín, M. T.; Marín, M.; Rama, R. J.; Álvarez, E.; Maya, C.; Molina, F.; Nicasio, M. C. Zero-Valent ML_2 Complexes of Group 10 Metals Supported by Terphenyl Phosphanes. *Chem. Commun.* **2021**, *57*, 3083–3086.
- (31) Martín, M. T.; Marín, M.; Maya, C.; Prieto, A.; Nicasio, M. C. Ni(II) Precatalysts Enable Thioetherification of (Hetero)Aryl Halides and Tosylates and Tandem C–S/C–N Couplings. *Chem. – Eur. J.* **2021**, *27*, 12320–12326.
- (32) Poater, A.; Cosenza, B.; Correa, A.; Giudice, S.; Ragone, F.; Scarano, V.; Cavallo, L. SambVca: A Web Application for the Calculation of the Buried Volume of N-Heterocyclic Carbene Ligands. *Eur. J. Inorg. Chem.* **2009**, *2009*, 1759–1766.
- (33) Clavier, H.; Nolan, S. P. Percent Buried Volume for Phosphine and N-Heterocyclic Carbene Ligands: Steric Properties in Organometallic Chemistry. *Chem. Commun.* **2010**, *46*, 841–861.
- (34) Falivene, L.; Cao, Z.; Petta, A.; Serra, L.; Poater, A.; Oliva, R.; Scarano, V.; Cavallo, L. Towards the Online Computer-Aided Design of Catalytic Pockets. *Nat. Chem.* **2019**, *11*, 872–879.
- (35) Gensch, T.; Gomes, G. d. P.; Friederich, P.; Peters, E.; Gaudin, T.; Pollice, R.; Jorner, K.; Nigam, A.; Lindner-D’Addario, M.; Sigman, M. S.; Aspuru-Guzik, A. A Comprehensive Discovery Platform for Organophosphorus Ligands for Catalysis. *J. Am. Chem. Soc.* **2022**, *144*, 1205–1217.
- (36) Standley, E. A.; Smith, S. J.; Müller, P.; Jamison, T. F. A Broadly Applicable Strategy for Entry into Homogeneous Nickel(0) Catalysts from Air-Stable Nickel(II) Complexes. *Organometallics* **2014**, *33*, 2012–2018.
- (37) Niemeyer, Z. L.; Milo, A.; Hickey, D. P.; Sigman, M. S. Parameterization of Phosphine Ligands Reveals Mechanistic Pathways and Predicts Reaction Outcomes. *Nat. Chem.* **2016**, *8*, 610–617.
- (38) Ge, S.; Hartwig, J. F. Highly Reactive, Single-Component Nickel Catalyst Precursor for Suzuki–Miyaura Cross-Coupling of Heteroaryl Boronic Acids with Heteroaryl Halides. *Angew. Chem., Int. Ed.* **2012**, *51*, 12837–12841.
- (39) Clevenger, A. L.; Stolley, R. M.; Aderibigbe, J.; Louie, J. Trends in the Usage of Bidentate Phosphines as Ligands in Nickel Catalysis. *Chem. Rev.* **2020**, *120*, 6124–6196.
- (40) West, M. J.; Watson, A. J. B. Ni vs. Pd in Suzuki–Miyaura Sp^2 – Sp^2 Cross-Coupling: A Head-to-Head Study in a Comparable Precatalyst/Ligand System. *Org. Biomol. Chem.* **2019**, *17*, 5055–5059.
- (41) Bajo, S.; Laidlaw, G.; Kennedy, A. R.; Sproules, S.; Nelson, D. J. Oxidative Addition of Aryl Electrophiles to a Prototypical Nickel(0) Complex: Mechanism and Structure/Reactivity Relationships. *Organometallics* **2017**, *36*, 1662–1672.
- (42) Greaves, M. E.; Humphrey, E. L. B. J.; Nelson, D. J. Reactions of Nickel(0) with Organochlorides, Organobromides, and Organiodides: Mechanisms and Structure/Reactivity Relationships. *Catal. Sci. Technol.* **2021**, *11*, 2980–2996.
- (43) PhJohnPhos was also subjected to these spectroscopic studies, and it was observed that it reacted with $Ni(COD)_2$ to form $Ni(PhJohnPhos)_2$. Single crystals of this complex were obtained directly from the reaction mixture, confirming its identity (see SI for more information).
- (44) Even for the ligands that were able to form ligated complexes, the conversions were generally low (<20%) as determined by NMR spectroscopy.
- (45) Velian, A.; Lin, S.; Miller, A. J. M.; Day, M. W.; Agapie, T. Synthesis and C–C Coupling Reactivity of a Dinuclear Ni^I – Ni^I Complex Supported by a Terphenyl Diphosphine. *J. Am. Chem. Soc.* **2010**, *132*, 6296–6297.
- (46) Herbert, D. E.; Lara, N. C.; Agapie, T. Arene C–H Amination at Nickel in Terphenyl-Diphosphine Complexes with Labile Metal-Arene Interactions. *Chem. – Eur. J.* **2013**, *19*, 16453–16460.
- (47) Nattmann, L.; Saeb, R.; Nöthling, N.; Cornella, J. An Air-Stable Binary $Ni(0)$ –Olefin Catalyst. *Nat. Catal.* **2020**, *3*, 6–13.
- (48) Lutz, S.; Nattmann, L.; Nöthling, N.; Cornella, J. 16-Electron Nickel(0)–Olefin Complexes in Low-Temperature $C(Sp^2)$ – $C(Sp^3)$ Kumada Cross-Couplings. *Organometallics* **2021**, *40*, 2220–2230.
- (49) Tran, V. T.; Li, Z.; Apolinar, O.; Derosa, J.; Joannou, M. V.; Wisniewski, S. R.; Eastgate, M. D.; Engle, K. M. $Ni(COD)(DQ)$: An Air-Stable 18-Electron Nickel(0)–Olefin Precatalyst. *Angew. Chem., Int. Ed.* **2020**, *59*, 7409–7413.
- (50) Similar results observed with 4-chlorobenzotrifluoride and 4-chloroanisole, though decomposition to Ni black was significantly greater, and additional paramagnetic species were observed.
- (51) Zhu, S.; Shoshani, M. M.; Johnson, S. A. Versatile (η^6 Arene)– $Ni(PCy_3)$ Nickel Monophosphine Precursors. *Chem. Commun.* **2017**, *53*, 13176–13179.
- (52) NMR analysis of recrystallized **1** in the absence of additional free ligand shows partial ligand dissociation in a 1:1 ratio with a new resonance by ^{31}P NMR, suspected to be the $L_2Ni(0)$ dimer of **i**. Addition of 2 equiv of free ligand to this solution does not decrease the intensity of the peak attributed the dissociation product, which appears to form irreversibly. However, addition of 2 equiv of free ligand to solid **1** prior to its dissolution results in no observed dissociation product, giving further experimental support of the intermediacy of **i**.
- (53) Jongbloed, L. S.; García-López, D.; van Heck, R.; Siegler, M. A.; Carbó, J. J.; van der Vlugt, J. I. Arene $C(Sp^2)$ –H Metalation at Ni^{II} Modeled with a Reactive $PONC_{ph}$ Ligand. *Inorg. Chem.* **2016**, *55*, 8041–8047.
- (54) Omer, H. M.; Liu, P. Computational Study of the Ni-Catalyzed C–H Oxidative Cycloaddition of Aromatic Amides with Alkynes. *ACS Omega* **2019**, *4*, 5209–5220.
- (55) Mangin, L. P.; Zargarian, D. C–H Nickelation of Aryl Phosphinites: Mechanistic Aspects. *Organometallics* **2019**, *38*, 1479–1492.
- (56) Mangin, L. P.; Zargarian, D. C–H Nickelation of Naphthyl Phosphinites: Electronic and Steric Limitations, Regioselectivity, and Tandem C–P Functionalization. *Organometallics* **2019**, *38*, 4687–4700.

- (57) Mangin, L. P.; Zargarian, D. C–H Nickellation of Phenol-Derived Phosphinites: Regioselectivity and Structures of Cyclo-nickellated Complexes. *Dalton Trans.* **2017**, *46*, 16159–16170.
- (58) Vabre, B.; Lambert, M. L.; Petit, A.; Ess, D. H.; Zargarian, D. Nickelation of PCP- and POCOP-Type Pincer Ligands: Kinetics and Mechanism. *Organometallics* **2012**, *31*, 6041–6053.
- (59) Vabre, B.; Deschamps, F.; Zargarian, D. Ortho Derivatization of Phenols through C–H Nickelation: Synthesis, Characterization, and Reactivities of Ortho-Nickelated Phosphinite Complexes. *Organometallics* **2014**, *33*, 6623–6632.
- (60) Volpe, E. C.; Chadeayne, A. R.; Wolczanski, P. T.; Lobkovsky, E. B. Heterolytic CH-Bond Activation in the Synthesis of Ni{(2-Aryl- κ^2)Pyridine- κ N}₂ and Derivatives. *J. Organomet. Chem.* **2007**, *692*, 4774–4783.
- (61) Chong, E.; Kampf, J. W.; Ariafard, A.; Cauty, A. J.; Sanford, M. S. Oxidatively Induced C–H Activation at High Valent Nickel. *J. Am. Chem. Soc.* **2017**, *139*, 6058–6061.
- (62) Given that approximately half of the Ni decomposes, it is feasible that the mechanism proceeds via a sacrificial bimolecular pathway and/or involves Ni(I)–aryl species.
- (63) Zhou, Y.-Y.; Hartline, D. R.; Steiman, T. J.; Fanwick, P. E.; Uyeda, C. Dinuclear Nickel Complexes in Five States of Oxidation Using a Redox-Active Ligand. *Inorg. Chem.* **2014**, *53*, 11770–11777.
- (64) Dible, B. R.; Sigman, M. S.; Arif, A. M. Oxygen-Induced Ligand Dehydrogenation of a Planar Bis- μ -Chloronickel(I) Dimer Featuring an NHC Ligand. *Inorg. Chem.* **2005**, *44*, 3774–3776.
- (65) Dürr, A. B.; Fisher, H. C.; Kalvet, I.; Truong, K.-N.; Schoenebeck, F. Divergent Reactivity of a Dinuclear (NHC)Nickel(I) Catalyst versus Nickel(0) Enables Chemoselective Trifluoromethyl-selenolation. *Angew. Chem., Int. Ed.* **2017**, *56*, 13431–13435.
- (66) Guven, S.; Kundu, G.; Weßels, A.; Ward, J. S.; Rissanen, K.; Schoenebeck, F. Selective Synthesis of Z-Silyl Enol Ethers via Ni-Catalyzed Remote Functionalization of Ketones. *J. Am. Chem. Soc.* **2021**, *143*, 8375–8380.
- (67) Payard, P.-A.; Perego, L. A.; Ciofini, I.; Grimaud, L. Taming Nickel-Catalyzed Suzuki-Miyaura Coupling: A Mechanistic Focus on Boron-to-Nickel Transmetalation. *ACS Catal.* **2018**, *8*, 4812–4823.
- (68) Thomas, A. A.; Denmark, S. E. Pre-Transmetalation Intermediates in the Suzuki-Miyaura Reaction Revealed: The Missing Link. *Science* **2016**, *352*, 329–332.
- (69) Thomas, A. A.; Wang, H.; Zahrt, A. F.; Denmark, S. E. Structural, Kinetic, and Computational Characterization of the Elusive Arylpalladium(II)Boronate Complexes in the Suzuki–Miyaura Reaction. *J. Am. Chem. Soc.* **2017**, *139*, 3805–3821.
- (70) Christian, A. H.; Müller, P.; Monfette, S. Nickel Hydroxo Complexes as Intermediates in Nickel-Catalyzed Suzuki–Miyaura Cross-Coupling. *Organometallics* **2014**, *33*, 2134–2137.
- (71) In computational studies, Espinet and coworkers found that THF could stabilize Ni(II) species with CyJohnPhos (see reference 27). Under the catalytic conditions, it is likely that solvent and/or water may bind to Ni(II) as an L-type ligand, which would also require the phosphine to adopt a low %V_{bur} conformation with the B ring rotated out of the coordination site. We have also computationally explored THF binding to Ni(0) intermediate **i**, which while energetically uphill by 3.6 kcal/mol, may be a relevant species with solvent quantities of THF (see SI).
- (72) The most stable conformations for CyJohnPhos during the transmetalation steps had %V_{bur} values a few percent above %V_{bur} (*min*) of 32%. In these structures, the unsubstituted B ring was positioned >3 Å above (or below) the Ni xy-plane (i.e., monodentate) with stabilizing C–H \cdots π interactions observed between the hydrogens of the Ni-bound aryl group and the π -face of the B ring. See SI for details.
- (73) Biscoe, M. R.; Barder, T. E.; Buchwald, S. L. Electronic Effects on the Selectivity of Pd-Catalyzed C–N Bond-Forming Reactions Using Biarylphosphine Ligands: The Competitive Roles of Amine Binding and Acidity. *Angew. Chem., Int. Ed.* **2007**, *46*, 7232–7235.
- (74) Düfert, M. A.; Billingsley, K. L.; Buchwald, S. L. Suzuki-Miyaura Cross-Coupling of Unprotected, Nitrogen-Rich Heterocycles: Substrate Scope and Mechanistic Investigation. *J. Am. Chem. Soc.* **2013**, *135*, 12877–12885.
- (75) Wolfe, J. P.; Buchwald, S. L. Nickel-Catalyzed Amination of Aryl Chlorides. *J. Am. Chem. Soc.* **1997**, *119*, 6054–6058.
- (76) Lavoie, C. M.; Stradiotto, M. Bisphosphines: A Prominent Ancillary Ligand Class for Application in Nickel-Catalyzed C–N Cross Coupling. *ACS Catal.* **2018**, *8*, 7228–7250.
- (77) Liu, R. Y.; Dennis, J. M.; Buchwald, S. L. The Quest for the Ideal Base: Rational Design of a Nickel Precatalyst Enables Mild, Homogeneous C–N Cross-Coupling. *J. Am. Chem. Soc.* **2020**, *142*, 4500–4507.
- (78) Lavoie, C. M.; MacQueen, P. M.; Rotta-Loria, N. L.; Sawatzky, R. S.; Borzenko, A.; Chisholm, A. J.; Hargreaves, B. K. V.; McDonald, R.; Ferguson, M. J.; Stradiotto, M. Challenging Nickel-Catalysed Amine Arylations Enabled by Tailored Ancillary Ligand Design. *Nat. Commun.* **2016**, *7*, 11073.
- (79) Clark, J. S. K.; Ferguson, M. J.; McDonald, R.; Stradiotto, M. PAd₂-DalPhos Enables the Nickel-Catalyzed C–N Cross-Coupling of Primary Heteroarylamines and (Hetero)Aryl Chlorides. *Angew. Chem., Int. Ed.* **2019**, *58*, 6391–6395.
- (80) Lavoie, C. M.; Tassone, J. P.; Ferguson, M. J.; Zhou, Y.; Johnson, E. R.; Stradiotto, M. Probing the Influence of PAd-DalPhos Ancillary Ligand Structure on Nickel-Catalyzed Ammonia Cross-Coupling. *Organometallics* **2018**, *37*, 4015–4023.
- (81) Zhang, S.; Li, X.; Sun, H. Selective Amination of Aryl Chlorides Catalysed by Ni(PMe₃)₄. *Dalton Trans.* **2015**, *44*, 16224–16227.
- (82) Hu, H.; Burlas, C. E.; Curley, S. J.; Gruchala, T.; Qu, F.; Shaughnessy, K. H. Effect of Aryl Ligand Identity on Catalytic Performance of Trineopentylphosphine Arylpalladium Complexes in N-Arylation Reactions. *Organometallics* **2020**, *39*, 3618–3627.
- (83) Malapit, C. A.; Borrell, M.; Milbauer, M. W.; Brigham, C. E.; Sanford, M. S. Nickel-Catalyzed Decarbonylative Amination of Carboxylic Acid Esters. *J. Am. Chem. Soc.* **2020**, *142*, 5918–5923.
- (84) Simon, C. M.; Dudra, S. L.; McGuire, R. T.; Ferguson, M. J.; Johnson, E. R.; Stradiotto, M. Identification of a Nitrenoid Reductive Elimination Pathway in Nickel-Catalyzed C–N Cross-Coupling. *ACS Catal.* **2022**, *12*, 1475–1480.
- (85) Till, N. A.; Tian, L.; Dong, Z.; Scholes, G. D.; MacMillan, D. W. C. Mechanistic Analysis of Metallaphotoredox C–N Coupling: Photocatalysis Initiates and Perpetuates Ni(I)/Ni(III) Coupling Activity. *J. Am. Chem. Soc.* **2020**, *142*, 15830–15841.
- (86) For BrettPhos, it is known with Pd that the ligand can adopt conformations wherein the 3-OMe of the A-ring is bound to the metal, adopting its minimum %V_{bur} (*min*) conformer of 35%. While we have not ruled out its possibility in Reaction IV, or in Ni catalysis more generally, this binding mode would also effectively make the ligand bidentate, as the OMe group fully occupies a second coordination site on the metal.